Enhancing Apoptosome Assembly via Mito-Biomimetic Lipid Nanocarrier for Cancer Therapy

Han, Huijie; Chen, Jie; Li, Jiachen; Correia, Alexandra; Bártolo, Raquel; Shahbazi, Mohammad-Ali; Teesalu, Tambet; Wang, Shiqi; Cui, Wenguo; Santos, Hélder A.

Published in:
Advanced Functional Materials

DOI:
10.1002/adfm.202305316

Publication date:
2023

Optimizing Interface Conductivity in Electronics

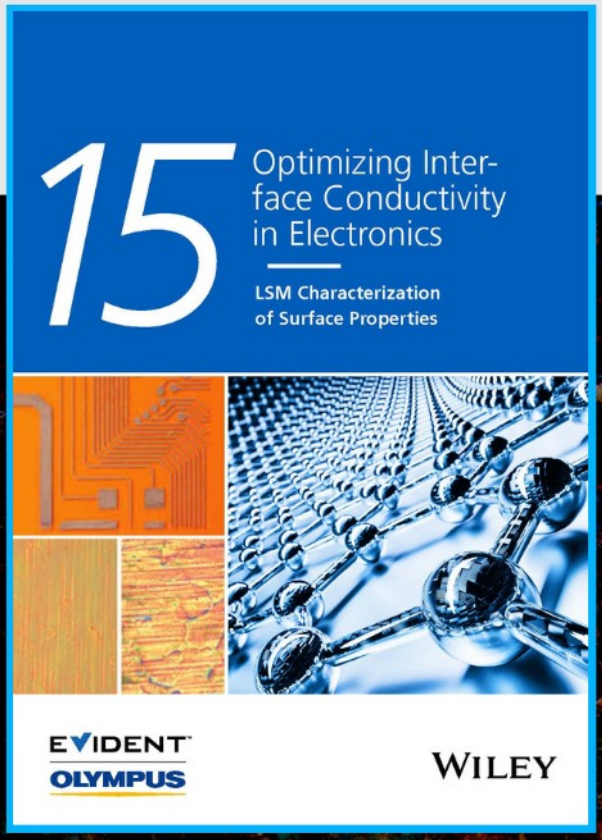

The latest eBook from Advanced Optical Metrology. Download for free.

Surface roughness is a key parameter for judging the performance of a given material's surface quality for its electronic application. A powerful tool to measure surface roughness is 3D laser scanning confocal microscopy (LSM), which will allow you to assess roughness and compare production and finishing methods, and improve these methods based on mathematical models.

Focus on creating high-conductivity electronic devices with minimal power loss using laser scanning microscopy is an effective tool to discern a variety of roughness parameters.

EVIDENT
OLYMPUS

WILEY

ADVANCED FUNCTIONAL MATERIALS
www.afm-journal.de

Enhancing Apoptosome Assembly via Mito-Biomimetic Lipid Nanocarrier for Cancer Therapy

Huijie Han, Jie Chen, Jiachen Li, Alexandra Correia, Raquel Bártolo, Mohammad-Ali Shahbazi, Tambet Teesalu, Shiqi Wang, Wenguo Cui,* and Hélder A. Santos**

Apoptosis is the natural programmed cell death process, which is responsible for abnormal cell clearance. However, many cancer cells develop various mechanisms to escape apoptosis through interrupting apoptosome assembly, which is a key step to initiate apoptosis. This promotes tumorigenesis and drug resistance, and thus, poses a great challenge in cancer treatment. Herein, a biomimetic lipid nanocarrier mimicking mitochondrial Cytochrome C (Cyt C) binding is developed. Cardiolipin, the major phospholipid of mitochondrial inner membrane, is introduced as the main component in biomimetic liposomal formulation. With the help of cardiolipin, Cyt C is sufficiently loaded in liposome based on electrostatic and hydrophobic interaction with cardiolipin. Lonidamine (LND) is added in hydrophobic phase of liposome to modulate the metabolic activity within cancer cells and sensitize the cells to Cyt C-induced apoptosis. The results suggest that LND reduces ATP level and creates favorable environment for Cyt C induced apoptosome assembly, exhibiting higher apoptosis level and anti-tumor efficacy in vitro and in vivo. The conjugation of a tumor-homing peptide, LinTT1, on the nanovesicle, increases the efficacy due to enhanced tumor accumulation. Overall, this biomimetic lipid nanocarrier proves to be an efficient delivery system with great potential of pro-apoptosis cancer therapy.

1. Introduction

Apoptosis is a programmed cell death occurring regularly to keep homeostatic balance of cell survival and death.[1] During intrinsic cell apoptosis, Cytochrome C (Cyt C) is released from mitochondrial intermembrane and binds to apoptotic protease-activating factor-1 (Apaf-1), triggering nucleotide exchange from dATP/ATP to dADP/ADP. Then seven Apaf-1-Cyt C complexes assemble into heptameric apoptosome.[2] Apoptosome is a vital oligomer protein complex in cell apoptosis, and the key mediator to activate the caspase-related signaling pathways. By recruiting pro-caspase 9 and triggering caspase 9 auto processing, apoptosome initiate a cascade of events, including effector caspase 3 and 7 activation, cytoplasmic endonuclease activation, nuclear disruption, cytoskeletal protein proteolysis and eventually cell death.[3]

The assembly of apoptosome determines cell fate during apoptosis, but cancer cells have developed various strategies to

H. Han, J. Chen, W. Cui, H. A. Santos
Department of Orthopaedics
Shanghai Key Laboratory for Prevention and Treatment of Bone and Joint Diseases
Shanghai Institute of Traumatology and Orthopaedics
Ruijin Hospital
Shanghai Jiao Tong University School of Medicine
Shanghai 200025, China
E-mail: wgcui@sjtu.edu.cn; h.a.santos@umcg.nl

H. Han, R. Bártolo, M.-A. Shahbazi, H. A. Santos
Department of Biomedical Engineering
University Medical Center Groningen
University of Groningen
Groningen 9713 AV, The Netherlands

The ORCID identification number(s) for the author(s) of this article can be found under https://doi.org/10.1002/adfm.202305316

DOI: 10.1002/adfm.202305316

H. Han, J. Li, R. Bártolo, M.-A. Shahbazi, H. A. Santos
W.J. Kolff Institute for Biomedical Engineering and Materials Science
University Medical Center Groningen
University of Groningen
Groningen 9713 AV, The Netherlands

A. Correia, S. Wang, H. A. Santos
Drug Research Program
Division of Pharmaceutical Chemistry and Technology
Faculty of Pharmacy
University of Helsinki
Helsinki FI-00014, Finland
E-mail: shiqi.wang@helsinki.fi

T. Teesalu
Laboratory of Cancer Biology, Institute of Biomedicine and Translational Medicine
Centre of Excellence for Translational Medicine
University of Tartu
Tartu 50411, Estonia

T. Teesalu
Cancer Research Center
Sanford-Burnham Medical Research Institute
San Diego, CA 92037, USA

escape apoptosis through apoptosome dysfunction. These strategies mainly include the inhibition of Cyt C release and the suppression of apoptosome assembly.[4] In a typical apoptotic process, Cyt C is released from pores on mitochondrial outer membrane (MOM) formed by pro-apoptotic proteins. However, many cancers have been reported to highly express anti-apoptotic proteins (like Bcl-2, Bcl-xl, and Mcl-1) to block MOM pore formation and Cyt C release.[5] As for the apoptosome suppression, it also reported that nucleotides such as ATP tended to bind cytosolic Cyt C, thus inhibiting Cyt C-Apaf-1 interaction and apoptosome assembly.[6] Besides, low expression or inactivation of Apaf-1 has been well observed in most cancers, mediated by heat shocking protein 27, 70, 90, etc.[7] Apoptosome dysfunction promotes both tumorigenesis and tumor resistance to standard therapies,[4] For example, in many human cancer tissues (acute leukemias, bladder cancer, prostate cancer, etc.), several anti-apoptosis molecules like prothymosin α, Aven, are overexpressed to prevent Apaf-1 oligomerization.[8] Besides, Cyt C deficiency has been found in association with greater docetaxel therapeutic resistance and faster prostate cancer recurrence in African-American patients.[9] Therefore, targeting apoptosome dysfunction and promoting apoptosome assembly is considered to be an efficient therapeutic strategy. However, there are few reports in this field. Recently, Wang et al. demonstrated that silencing Apaf-1 binding Noncoding RNA (ABL) significantly enhanced chemotherapy sensitivity through relieving apoptosome assembly block, which indicated the potential of apoptosome-based cancer therapy.[10]

Intracellular delivery of Cyt C is a promising approach to enhance apoptosome formation and pro-apoptosis, since the exogenous Cyt C delivered into the cytosol compensated the insufficient release of endogenous Cyt C. Many nanocarriers, including silica nanoparticles (NPs), lipid-apolipoprotein, poly (lactic-co-glycolic acid), and hyaluronic acid nanogels have been reported to deliver Cyt C for cancer therapy.[11] However, these Cyt C delivery nanoplatforms have limited therapeutic efficiency both in vitro and in vivo, although sufficient Cyt C loading and release have been achieved at tumor sites via stimuli-responsive release system.[12b,h,i] Thus, it is assumed that the cytosolic delivery of Cyt C is not enough to induce significant apoptotic effects, and new drug combination strategies to sensitize cancer cells to apoptosis should be considered to achieve better therapeutic outcomes.

In addition to insufficient intracellular Cyt C, suppressed apoptosome assembly in cancer cells is another factor limiting the apoptosis according to the mechanisms discussed above. Thus, it is hypothesized that the combination of Cyt C delivery with enhanced apoptosome assembly would lead to synergistic pro-apoptosis effects (**Scheme 1**). To test this hypothesis, herein, we designed a lipid nanocarrier co-delivering Cyt C with Lonidamine (LND), an antiglycolytic drug, and hexokinase II (HK II) inhibitor. Since most tumor cells rely on aerobic glycolysis to generate ATP, the inhibition of glycolysis by LND deprives intracellular ATP, and thus, promotes Cyt C binding with Apaf-1 to form apoptosome assemblies.[12] Lipid nanocarriers were chosen for Cyt C and LND co-delivery because of their biocompatibility, biodegradability, enhanced pharmacokinetics, and the capability of co-encapsulating drugs with different polarities and solubilities.[13] Furthermore, lipid nanocarrier refers to mitochondrial Cyt C anchoring way, cardiolipin (CL) was introduced in nanocarrier formulation, mimicking the natural mitochondrial-derived vesicles, where the Cyt C-CL complex anchors on the mitochondrial membranes. In physiological conditions, Cyt C binds to CL via electrostatic and hydrophobic interactions with high affinity.[14] Kinnuen et al. first revealed that Cyt C binds to CL through two binding sites, named as A site and C site.[15] The A site of Cyt C has abundant lysine residues and interacts with phosphate groups of CL electrostatically, while one acyl chain of CL is inserted into hydrophobic channel of Cyt C at C site.[16] In addition to high loading capability, it is expected the biomimetic Cyt C loading could maintain Cyt C conformation and keep protein activity.

In this study, CL-containing biomimicking lipid nanovesicles were developed. First, lipid formulations were fabricated, characterized, and optimized. Then a tumor homing peptide, LinTT1 (AKRGARSTA), was conjugated to the optimized formulation, aiming at enhancing the tumor targeting efficiency. According to literature, LinTT1 is identified as homing to p32 protein (or gC1qR), which is significantly overexpressed in many malignant and stromal cancer cells including 4T1 and MDA-MB-231 breast cancer cells.[17] The anti-tumor and pro-apoptotic effects of the formulation with or without LinTT1 were evaluated in breast cancer cells, 4T1 and MDA-MB-231. Particularly, apoptotic marker proteins (Apaf-1, Cyt C) involved in the apoptosome formation were characterized to validate our hypothesis and reveal the mechanisms of pro-apoptotic effects. Furthermore, the synergetic anti-tumor effect of drug combination in vivo was also investigated in a 4T1 breast cancer-bearing mouse model.

2. Results and Discussion

2.1. Optimization and Characterization of the Lipid Nanocarriers

First, the biomimicking lipid nanovesicles were prepared by a standard extrusion method,[18] with different CL contents. As shown in **Figure 1**a–c, the size and polydispersity (PDI) did not show major changes, while the zeta-potential reduced significantly along with increased CL content, due to the negative charged head of CL. When these formulations were loaded with Cyt C and loading efficiency was quantified by UV-absorbance (Figure S1, Supporting Information), it was found that there was almost no Cyt C loading without CL while increasing CL content led to a significant Cyt C loading (Figure 1d). It is hypothesized that Cyt C was loaded in liposome based on Cyt C-CL interaction, similar to the structure in mitochondrial membranes.[19] Despite the efficient loading of Cyt C, it was also found that liposomes with CL content over 10% led to moderate cytotoxicity (Figure S2, Supporting Information), so 10% CL lipo was finally determined in the liposome formulation. The CL liposome was in unilamellar and spheroid-like shape (Figure 1e), the typical structure of a liposome.[20]

Then the lipid formulation was loaded with LND (Figure 1f). The LND loading degree gradually increased along with increasing LND feeding ratio. When LND content increased from 11.1 to 12.5% (wt.%, compared with lipids), the LND loading degree rise from 8.3 to 9.3%. However, when further increasing LND content to 16.7%, the loading degree only increased slightly to 9.6%, suggesting that it may already reach the plateau. The loading of LND did not cause significant changes in liposome size and zeta potential (Table S1, Supporting Information). Therefore,

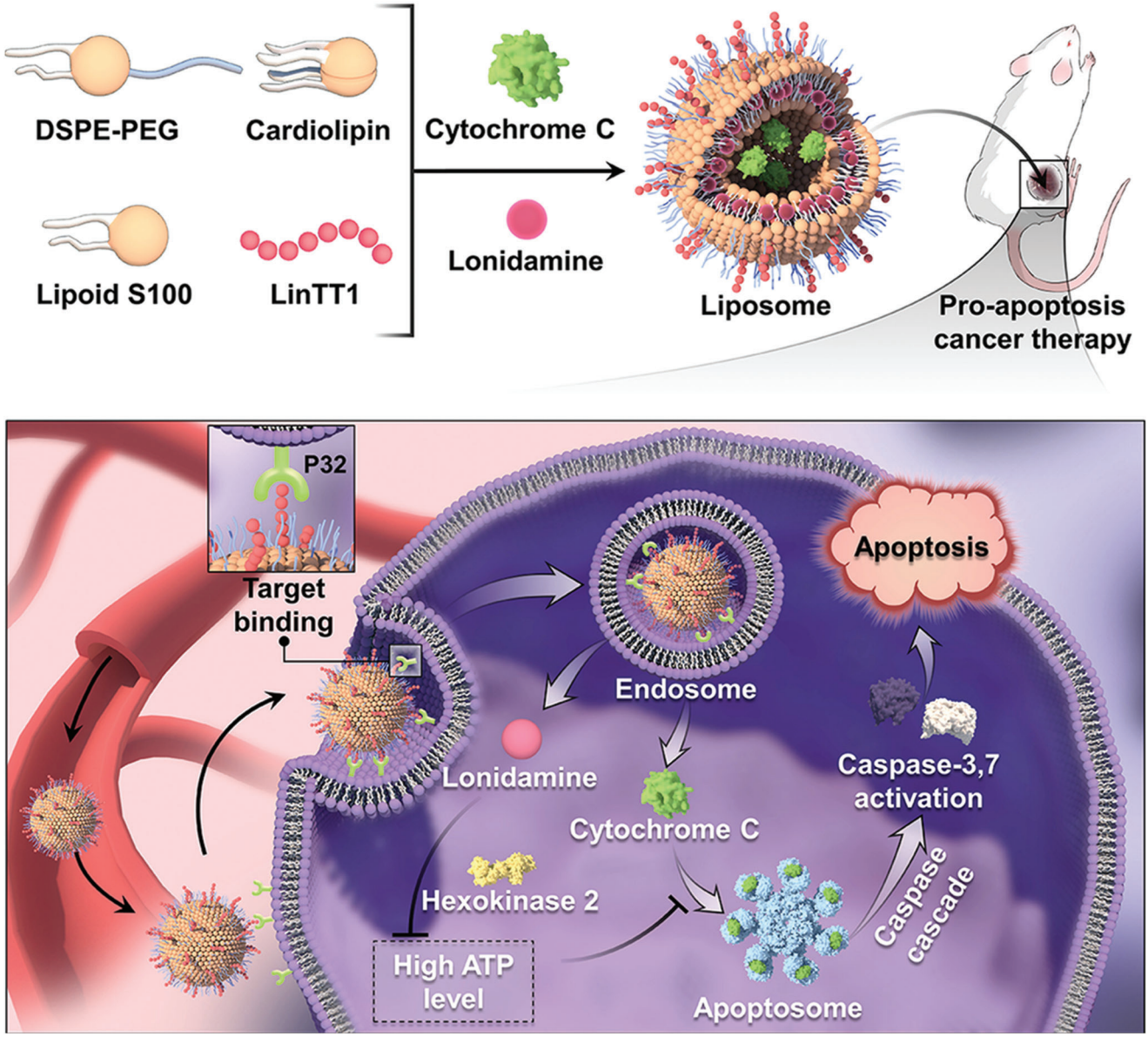

Scheme 1. Nanoparticle design and schematic illustration of biomimetic lipid nanocarrier enhancing apoptosome assembly in breast cancer therapy.

the LND content of 16.7% (wt.%) was chosen in final formulation based on sufficient LND loading and integral liposome structure (Figure S3, Supporting Information).

After the optimization of Cyt C and LND loading separately, we proceeded with dual-drug loaded nanoformulation. Similarly, the average size, PDI, zeta-potential, and morphology of the final formulation were characterized and compared with single drug loading or empty liposomes (Figure 1e,g–i; Figure S3, Supporting Information). The average diameter of different liposomes loaded with Cyt C and/or LND ranged from 121.5 to 131.8 nm. All liposomes were monodispersed with narrow size distribution (PDI < 0.2). The suitable size and uniform size distribution indicated the potential for systemic administration.[21] The zeta-potential of blank liposome (CL lipo) was −28.7 ± 3.0 mV, and the loading of Cyt C demonstrated no difference in zeta-potential (−27.6 ± 1.7 mV) although Cyt C was positive-charged. It may indicate that Cyt C was mainly loaded inside instead of on the surface of liposomes.

Finally, carboxyfluorescein (FAM) labeled LinTT1 peptide was conjugated onto the liposome's surface through thiol-maleimide reaction between distearoyl phosphoethanolamine (DSPE)-PEG-maleimide and the cysteine residual in LinTT1. To characterize the LinTT1 conjugation, FAM-LinTT1 standard curve was used (Figure S4, Supporting Information), and the conjugated LinTT1 molar ratio was calculated as 0.2% of total lipid. Conjugation of LinTT1 on liposomes was also affirmed by the zeta-potential changes, from −29.1 ± 0.6 to −25.2 ± 0.7 mV. This is consistent with previous reports,[17c] since LinTT1 has positively charges residuals in its sequence.

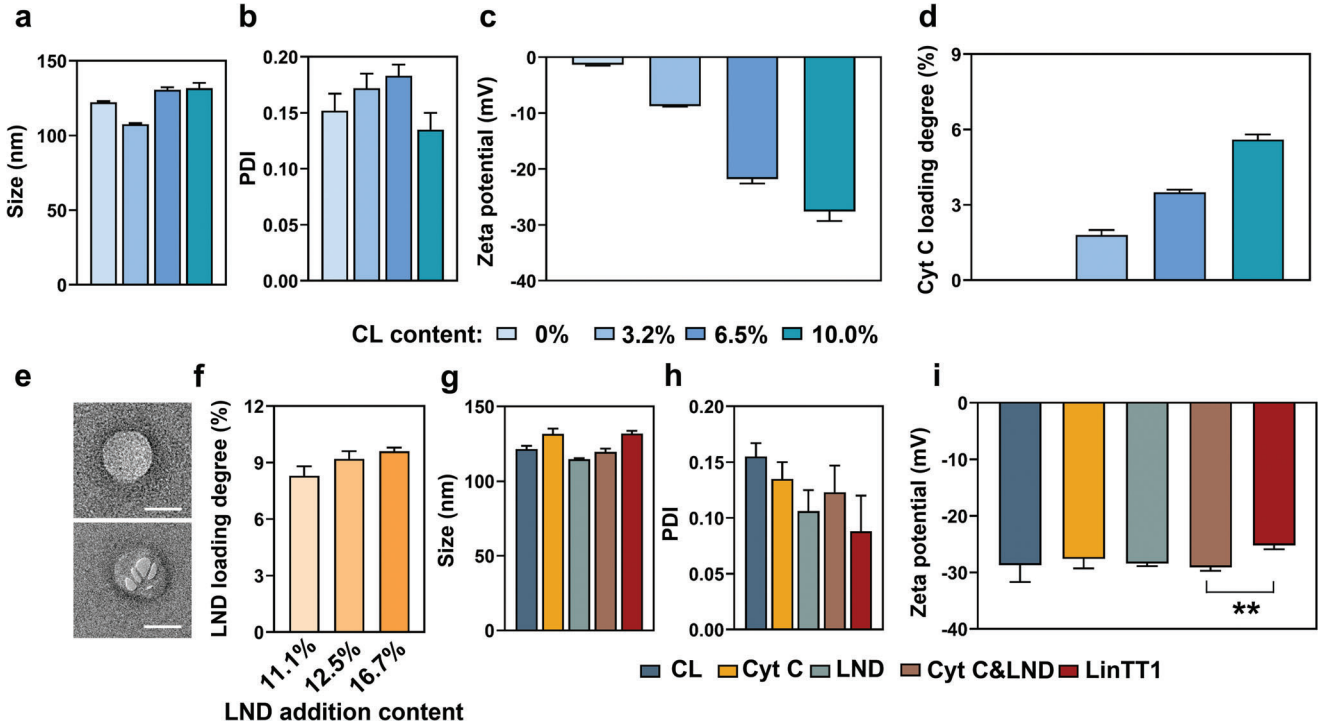

Figure 1. Physicochemical characterizations of liposomes. a,b,c) Size, PDI, and zeta-potential of Cyt C liposomes with different CL content in molar ratio. d) Cyt C loading degree (wt.%) in Cyt C liposomes with different CL content. e) The TEM image of CL liposome (Above) and Cyt C&LND liposome (Below). f) LND loading degree (wt.%) in LND liposomes. g,h,i) Size, PDI, and zeta-potential of all liposome formulations. (TEM: transmission electron microscopy; CL: CL containing blank liposome; Cyt C: Cyt C loaded liposome; LND: LND loaded liposome; Cyt C&LND: Cyt C and LND co-loaded liposome; LinTT1: LinTT1 modified Cyt C&LND co-loaded liposome). Results are shown as mean ± SD, $n = 3$. (Scale bar: 100 nm). The statistical test was performed by Student's *t*-test. $^{**}p < 0.01$.

2.2. Drug Loading, Release Profile, and Stability Studies

After the liposome formulation optimization, the loading degree of Cyt C and LND was characterized in the liposomal formulations (**Figure 2**a,b). The Cyt C loading was 5.6%, 6.2%, and 6.0% in Cyt C lipo, drug co-loading lipo, and LinTT1 lipo, respectively, while LND loading was 9.6%, 9.0%, and 8.5% in LND, drug co-loading lipo, and LinTT1 lipo. The co-loading procedures and LinTT1 conjugation did not change the Cyt C contents in the final formulation, but a slight decrease of LND loading ($p < 0.05$) was shown from LND, Cyt C&LND to LinTT1 lipo, possibly due to LND leakage during liposome extrusion and LinTT1 modification reaction.

The in vitro release profile of LND was evaluated in pH 7.4 and pH 5.5, phosphate buffer saline (PBS) buffer containing 10% fetal bovine serum (FBS) (Figure 2c,d; Figure S5, Supporting Information). FBS was introduced in release medium to mimic the cellular conditions. All free LND released out from dialysis bag within 2 h (Figure S5, Supporting Information). Regarding LND-loaded liposomes, LND release was more sustained and reached 80% in 10 h, which makes it possible to achieve sufficient drug accumulation in the tumor tissue. The release profile in pH 7.4 and pH 5.5 buffer conditions did not have major differences, suggesting the release was simply due to the LND diffusion from the nanocarrier. LND release in the co-loaded Cyt C&LND liposome owned the similar release profile, indicating that Cyt C did not interfere with LND release in the liposome system.

Liposome stability was also studied in 50% plasma solution to simulate the in vivo physiological environment (Figure 2e). After intravenous injection, liposomes interact with plasma protein, and protein corona forms on surface of liposome, which may cause nanoparticle aggregation.[22] To evaluate the colloidal stability, the size and distribution of all liposome formulations were tracked over 72 h. The results in Figure 2e showed that our liposomes had stable size distribution in 50% plasma solution within 24 h incubation, although there was significant size increase after 48 and 72 h incubation, possibly due to the dynamic protein corona formation. It is hypothesized that soft corona was first formed on liposome by exchangeable plasma proteins dynamically, and the soft corona was unstable and revisable without significant size difference.[23] Then after long time incubation, high-affinity protein attached on liposome and hard corona formed irreversibly,[23] and thus, the particle size increased from ≈120 to ≈220 nm for all liposomes. This indicated that the liposome formulations were stable in human plasma without clear aggregation within 72 h.

In addition to colloidal stability, the conformation of Cyt C was also studied. Both free Cyt C and Cyt C lipo samples were characterized by circular dichroism (CD) spectroscopy (Figure 2f,g). The far-ultraviolet (UV) region (190–260 nm) in CD revealed secondary structure of Cyt, including α-helical and β-sheet, turn, and random coil. Changes in backbone orientation of Cyt C were recognized[24] after loading in the CL-containing liposomes. The negative bands at 222 nm (n–π^* transition) decreased and

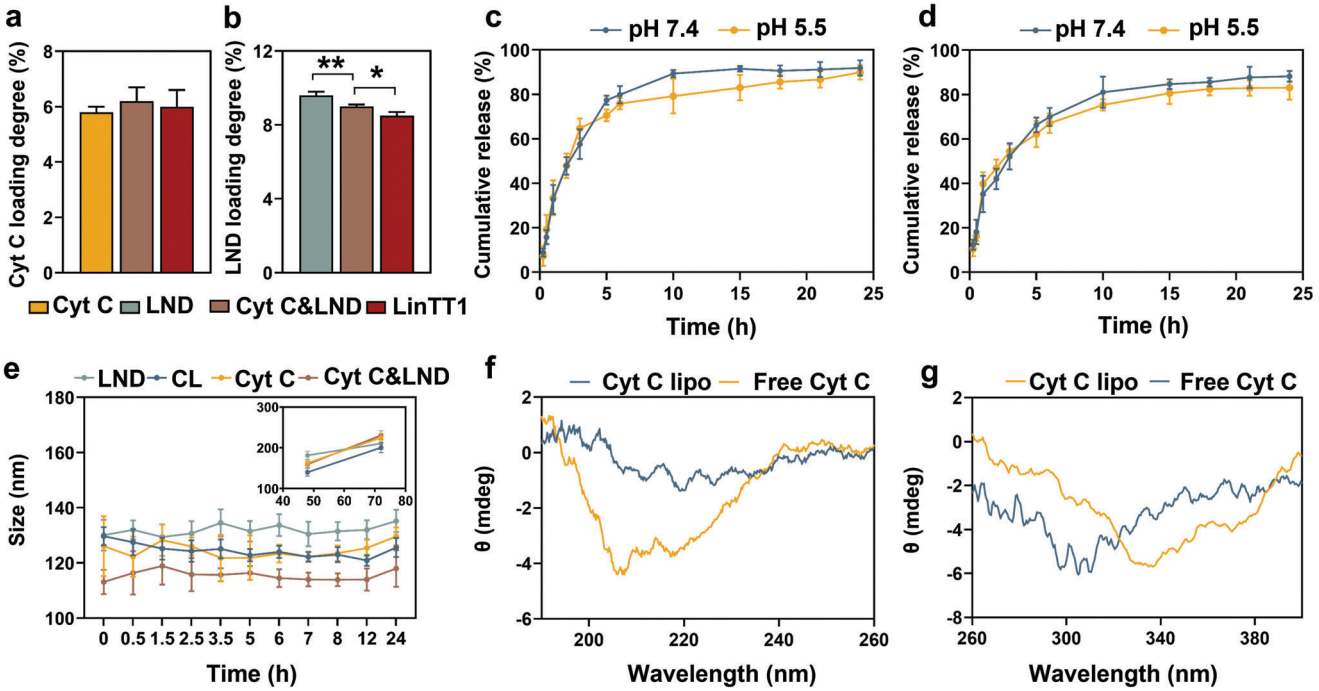

Figure 2. Loading, release profile and stability of lipid formulations. a,b) Cyt C and LND loading degree in different liposomes. c,d) LND release profile in PBS of pH 7.4 and pH 5.5 (containing 10% FBS) in LND liposome, and Cyt C&LND liposome, respectively. e) The colloidal stability of liposomes in 50% human plasma/0.9% NaCl at 37 °C. f,g) Circular dichroism spectra of free Cyt C and Cyt C loaded liposomes. Results are shown as mean ± SD, $n = 3$. The statistical test was performed by Student's t-test. $^{*}p < 0.05$, $^{**}p < 0.01$.

indicated the decreased of α-helical structure after interacting with CL. Besides, the middle UV region (260–400 nm) revealed the tertiary structure of Cyt C changed after CL interaction. The alternation of Cyt C confirmation was due to Cyt C-CL binding based on hydrophobic and electrostatic force as explored before.[25] This confirmed the high loading capacity in our nanocarrier originated from the biomimetic Cyt C-CL interactions.

2.3. In Vitro Anti-Tumor Efficacy Mediated by Apoptosis

The in vitro anti-tumor efficacy of the nanocarriers was studied in mouse-derived breast cancer cells (4T1), and human-derived triple negative breast cancer cells (MDA-MB-231). As shown in **Figure 3**a, CL lipo exhibited no cytotoxicity after 24 and 48 h incubation up to 1 mg mL^{-1} concentration. It was also noticeable that free Cyt C had very little anti-tumor effect up to 1 mg mL^{-1} (Figure S6, Supporting Information) because only intracellular Cyt C promoted apoptosis. At 0.25 mg mL^{-1}, Cyt C loaded liposomes reduced 4T1 cell viability to 76.3% after 24 h incubation, and further to 56.3% after 48 h incubation, demonstrating the liposomal formulation of Cyt C exhibited anti-tumor effects due to the intracellular delivery of Cyt C.

The therapeutic effect of Cyt C and LND combination was also studied (Figure 3a). The single drug-loaded liposome had limited toxicity on both 4T1 and MDA-MB-231 cell after 24 h incubation. However, Cyt C and LND co-loaded liposomes showed remarkable synergistic effect on both cells. MDA-MB-231 cell viability reduced from 97.2% (Cyt C lipo) and 80.4% (LND lipo), to 55.8% at 0.25 mg mL^{-1} after 24 h. The longer incubation time led to more significant anti-tumor effects, with a further decrease in cell viability to 29.4% after 48 h. The LinTT1 modification of liposome improved anti-tumor efficacy based on LinTT1 targeting effect and consequently higher liposome uptake.[26] Such enhanced in vitro anti-tumor effect after LinTT1 modification was observed in both breast cancer cell lines.

Then the mechanism behind Cyt C and LND-induced cell death was further studied. The apoptosis level of 4T1 cells treated with different liposomes was characterized by Annexin V/PI staining (Figure 3b; Figure S7, Supporting Information). The early and late-stage apoptosis level of 4T1 cells agreed with the cytotoxicity data in all liposome groups. The higher toxicity of liposome, the higher level of early and late-stage apoptosis (Figure 3b), indicating that the reduced cell viability was correlated with apoptosis. The Cyt C and LND combination statistically significantly increased early apoptosis level from 14.7% (Cyt C lipo), 29.6% (LND lipo) to 51.1% (Cyt C&LND lipo), corresponding with higher cell toxicity (Figure 3a). The LinTT1 modification further improved early apoptosis from 51.1% to 59.5%, probably owing to higher uptake of Cyt C and LND.

Since anti-tumor effect of Cyt C&LND liposome was accompanied with high apoptosis level, the mechanism behind the pro-apoptotic effects of Cyt C and LND was explored. We first investigated the apoptosome assembly formation in different treatment groups (Figure 3c), which is the key event during apoptosis. We separated apoptosomes from monomeric Apaf-1 protein by size exclusion chromatography (SEC) and used Western Blot to quantify the Apaf-1 level in the separated cell lysate fractions following literature-reported methodologies.[27] In

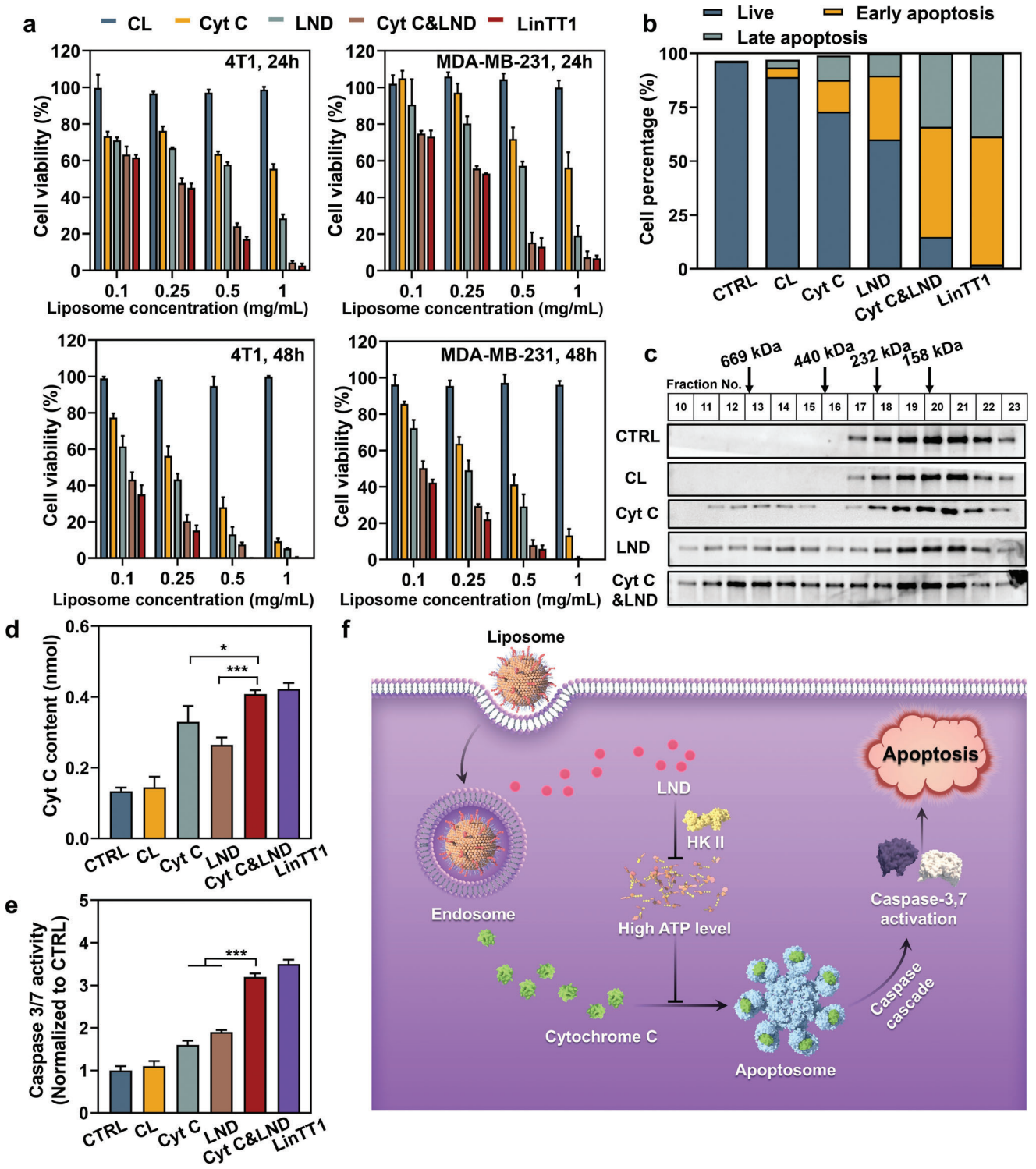

Figure 3. In vitro anti-tumor efficacy of all liposome formulations. a) The cytotoxicity of different liposomes treated 4T1 and MDA-MB-231 cells after 24 and 48 h incubation at different concentrations. b) Apoptosis level of different liposomes treated 4T1 cells (0.25 mg mL^{-1}, 48 h) based on annexin V-FITC/PI staining. c) Apoptosome level of different liposomes treated 4T1 cell (0.25 mg mL^{-1}, 24 h) by Apaf-1 Western Blot analysis. d) Cyt C content per 10 000 cells (nmol) of different liposomes treated 4T1 cell (0.25 mg mL^{-1}, 24 h). e) Caspase 3/7 activity of different liposomes treated 4T1 cell (0.25 mg mL^{-1}, 24 h). f) Scheme of mechanism on Cyt C and LND combination in apoptosis. Results are shown as mean ± SD, $n = 3$. The statistical test was performed by Student's *t*-test, $^{*}p < 0.05$, $^{***}p < 0.001$.

control (CTRL) and CL lipo group, there was no apoptosome formation, as the Apaf-1 bands did not present in the fractions above 440 kDa, and only showed in fractions ≈158 kDa, corresponding to Apaf-1 monomers. After Cyt C lipo and LND lipo treatment, we could clearly identify Apaf-1 bands in the fractions above 440 kDa, indicating successful Apaf-1 assembly into oligomers and apoptosomes. Cyt C and LND combination enhanced apoptosome formation because the Apaf-1 level in oligomer fractions (above 440 kDa) was higher than Cyt C lipo and LND lipo. The higher level of apoptosome formation in the dual-drug loaded liposome treatment group was consistent with the elevated apoptosis (Figure 3b).

To further investigate the underlying mechanisms of enhanced apoptosome assembly, we explored the effects of our liposomal formulations on the major components of apoptosomes, cytoplasmic Cyt C and Apaf-1. The Cyt C content in the cytosol (Figure 3d) after different liposomal formulation treatment was quantified based on the standard curve (Figure S8, Supporting Information). There was baseline level cytoplasmic Cyt C (0.13 nmol per 10 000 cells) in CTRL group, probably due to the mechanical damage during cytoplasm extraction. After Cyt C lipo treatment, the cytoplasmic Cyt C increased significantly to 0.33 nmol, indicating the successful Cyt C intracellular delivery. LND lipo also elevated Cyt C level based on its pro-apoptosis effect followed by Cyt C release from mitochondria.[28] The Cyt C and LND combination augmented Cyt C level to 0.41 nmol based on both intracellular Cyt C delivery and Cyt C release from mitochondria. The Apaf-1 expression level, however, was similar in all liposome groups and was not altered by either Cyt C or LND lipo treatment (Figure S9, Supporting Information). These results indicated that Cyt C and LND co-loaded liposomes promoted apoptosome assembly by delivering Cyt C to the cytosol without changing Apaf-1 expression.

In addition to the available Cyt C and Apaf-1 in the cytosol, the apoptosome assembly process is also affected by regulatory signaling molecules, such as ATP.[2a,4] The abnormal glycolysis and high ATP level within tumor cells inhibited apoptosome assembly and the subsequent apoptosis. Thus, we hypothesized that LND as a glycolysis inhibitor, could facilitate apoptosome formation by metabolic sensitization. To verify this hypothesis, we tested the ATP level in different treatment groups. As shown in Figure S10 (Supporting Information), LND containing lipo treatment had stronger ATP inhibition than Cyt C lipo at the same liposome concentration, decreasing ATP level from 92.1% to 60.8% in 4T1 cell at 0.25 mg mL^{-1} for 24 h, while Cyt C lipo had limited ATP reduction up to 1 mg mL^{-1}. According to literature, the ATP deprivation ability of LND may owe to hexokinase inhibition ability and following glycolysis suppression.[29]

Finally, we investigated effector caspases (Caspase 3/7 activity) (Figure 3e), to evaluate the downstream events in the apoptotic pathway. Consistent with the apoptosome level, caspase 3/7 activity of Cyt C and LND lipo elevated from 1.6-fold and 1.9-fold (normalized to CTRL) to 3.2-fold, demonstrating the higher apoptosis level after Cyt C and LND combinational delivery. Altogether, these mechanistic insights revealed that our liposomal formulation co-delivering Cyt C and LND could achieve a synergistic effect following potential mechanism in Figure 3f. Specifically, Cyt C and LND lipo could deliver exogenous Cyt C into the cytoplasm to relieve the intrinsic Cyt C deficiency in tumor cells. Meanwhile, the LND delivered inhibited tumor glycolysis and reduced intracellular ATP, promoting apoptosomes formation, and activated the caspase cascade accordingly. The combinational delivery of Cyt C and LND by our liposomal formulation achieved more significant apoptosis on breast cancer cells than either Cyt C lipo or LND lipo, and also much higher cytotoxicity in vitro.

2.4. Tumor Homing Ability of LinTT1 Lipo both In Vitro and In Vivo

To enhance the tumor accumulation and targeting capability of our liposomes, we conjugated LinTT1, a tumor homing peptide, on the liposomal surface. According to the literature, LinTT1 peptide has been identified to target p32 protein that was overexpressed in breast cancer cells.[30] Furthermore, p32 was also overexpressed by other cells in the tumor microenvironment, such as vascular endothelial cells and tumor-associated macrophages, imparting LinTT1 penetrating ability in tumor tissue.[17b] The targeting capability of liposomes with or without LinTT1 was studied both in vitro and in vivo (**Figure 4**).

The cellular uptake of LinTT1 lipo in 4T1 was studied qualitatively and quantitatively (Figure 4a,e). The liposome uptake after 1 and 3 h incubation was visualized by confocal microscopy (Figure 4a). Compared with bare lipo, LinTT1 lipo exhibited more intense and more dense fluorescence in 4T1 cytoplasm after 1 and 3 h incubation, indicating more liposome uptake in LinTT1 lipo group. The enhanced LinTT1 lipo uptake was also observed in MDA-MB-231 cells after 1 and 3 h incubation, with the same trend of 4T1 cellular uptake (Figure S11, Supporting Information). From the flow cytometry analysis, it was clear that LinTT1 modification markedly increased liposome uptake after 1 and 3 h incubation (Figure 4e), since the proportion of FAM-positive cells was higher in LinTT1 lipo, but the gap was narrowed with longer incubation time. This indicated that LinTT1 promoted liposome uptake in 4T1 cells during the early stage of incubation.

The biodistribution of LinTT1 lipo and bare liposomes was also studied in 4T1 bearing mice (Figure 4b–d,f,g) to verify the in vivo tumor targeting capability. LinTT1 lipo group exhibited statistically significantly faster and stronger Cyanine 5.5 fluorescence accumulation (Figure 4b,f) after intravenous injection. After 1 h injection, LinTT1 lipo had accumulated in tumor tissue (shown in blue circle), with markedly higher fluorescence intensity than bare lipo group. In contrast, bare lipo only showed fluorescence accumulation around tumor instead of inside the tumor. After 4 and 24 h injection, there was still a statistically significant difference in LinTT1 and bare lipo accumulation in tumor, and the gap seemed not shrinking over time. This indicated the tumor homing ability of LinTT1 lipo formulation in vivo.

All organs and tumors were collected after 24 h injection. Although most lipo were retained in liver (Figure 4c,g), the LinTT1 lipo tumor accumulation was on average 1.4-fold higher than the bare lipo. Besides, there were no clear difference between bare and LinTT1 lipo distribution in heart, spleen, kidney, and lung (Figure 4g). The stronger and quicker LinTT1 lipo accumulation in tumor led to enhanced drug accumulation in tumor and could promote therapeutic effects of drug-loaded liposomes.

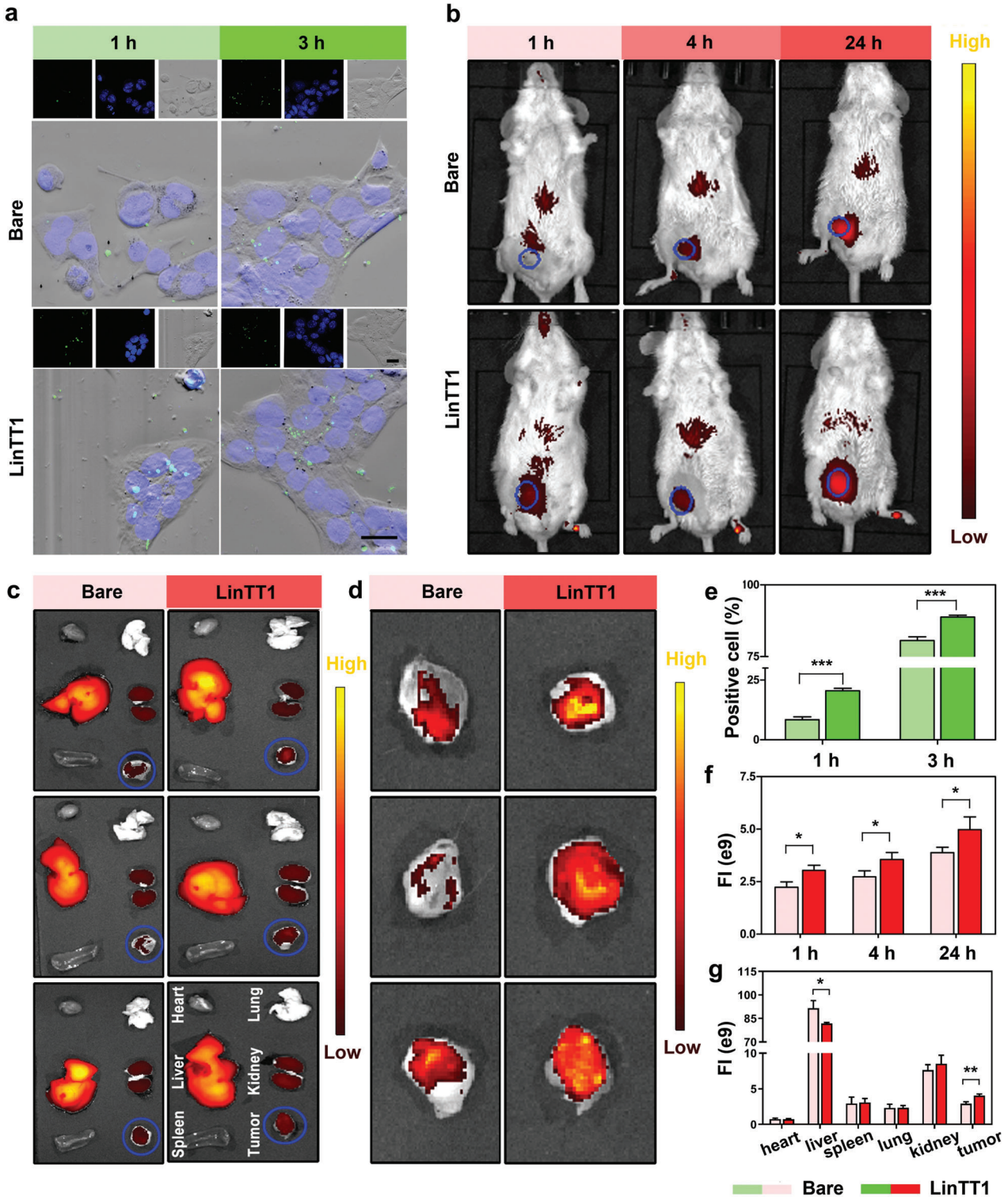

Figure 4. Tumor homing ability of LinTT1 liposomes in vitro and in vivo. a) Qualitative analysis of 4T1 cellular uptake by confocal microscope. 0.2 mg mL^{-1} of liposome were incubated with cells at 37 °C for 1 and 3 h. Nucleus was stained with DAPI (Blue), bare and LinTT1 functionalized liposome was labeled with FAM (Green). b) In vivo fluorescence images of bare and LinTT1 lipo biodistribution in 4T1 tumor bearing mice qualitatively. c,d) Ex vivo fluorescence images of organs (heart, live, spleen, lung, kidney) and tumors, and of tumors alone after 24 h injection qualitatively. e) Quantitative analysis of 4T1 cellular uptake by flow cytometry. f) In vivo fluorescence of bare and LinTT1 lipo biodistribution in 4T1 tumor bearing mice quantitatively. g) Ex vivo fluorescence of organs (heart, live, spleen, lung, kidney) and tumors after 24 h injection quantitatively. FI means fluorescence intensity. Tumors were circled in blue. Results are shown as mean ± SD, $n = 3$. (Scale bar: 20 μm). The statistical test was performed by Student's *t*-test. $^{*}p < 0.05$, $^{**}p < 0.01$, $^{***}p < 0.001$.

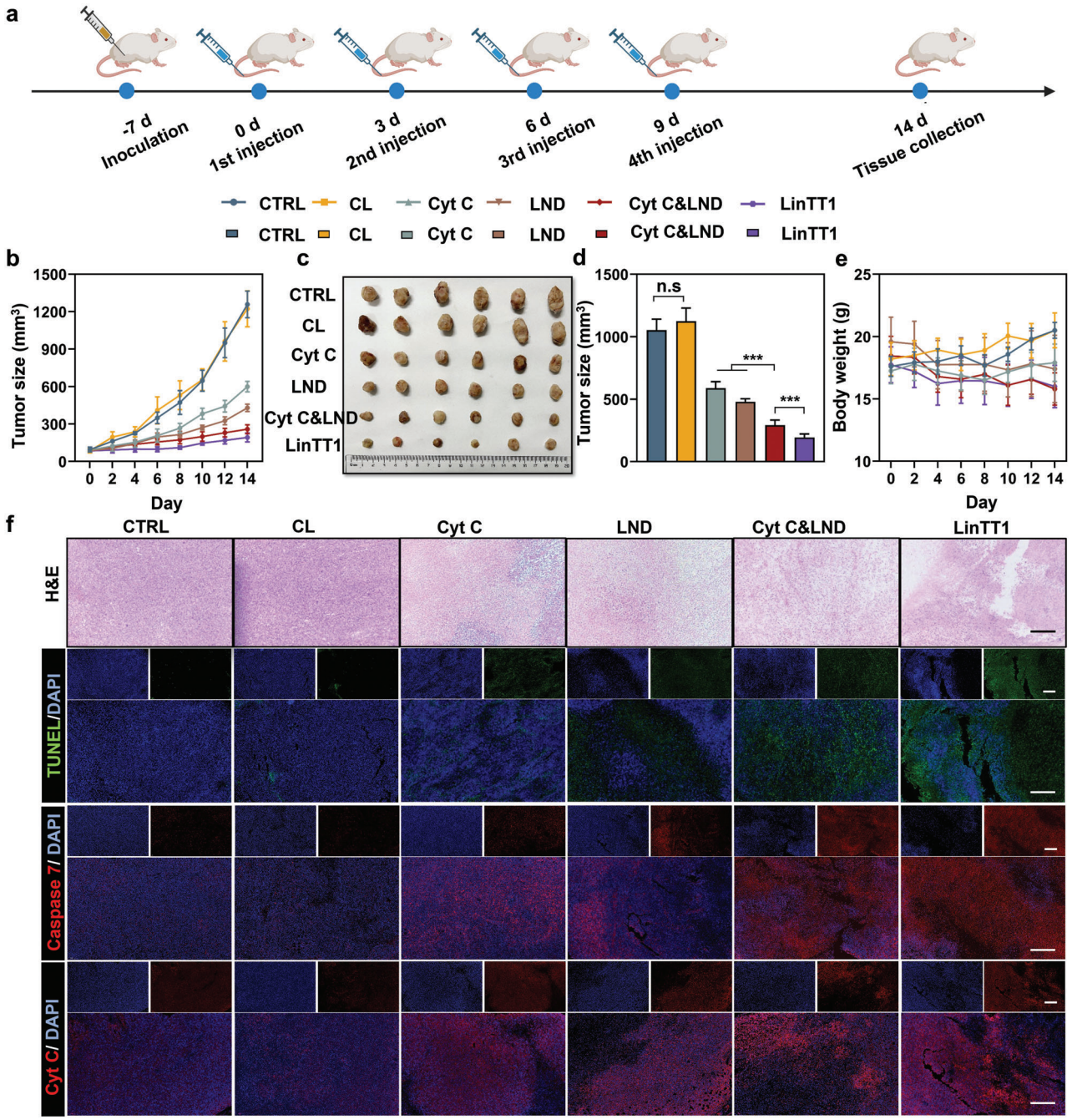

Figure 5. In vivo therapeutic efficacy on 4T1-bearing mice after treatment with different liposome formulations (Cyt C dosage of 1 mg kg^{-1}, LND dosage of 5 mg kg^{-1}, $n = 6$). a) Experimental schedule for Cyt C and LND combination therapy. b) Average tumor volume in vivo during 14 d treatment. c) Photograph of extracted tumor after 14 d treatment. d) Average tumor volume measured ex vivo after 14 d treatment. e) Average body weight of mice during 14 d treatment. f) H&E staining, TUNEL staining, Cyt C staining, Caspase-7 staining of tumors in different groups after 14 d treatment. Cell nuclei were stained with DAPI (Blue). Results are shown as mean ± SD, $n = 6$ (Scale bar: 200 μm). The statistical test was performed by Student's *t*-test. $^{***}p < 0.001$.

2.5. In Vivo Anti-Tumor Efficacy Evaluation

The anti-tumor efficacy study was conducted on xenograft 4T1 tumor-bearing mice (**Figure 5**). The experimental timeline is shown in Figure 5a. When comparing with Cyt C lipo and LND lipo, the Cyt C and LND co-loaded lipo group showed statistically significant tumor ablation and tumor growth inhibition (Figure 5b–d; Figure S12, Supporting Information). The average tumor size increased from 92.3 to 258.7 mm^3 after 14 d treatment, while the final tumor size in Cyt C lipo and LND lipo group was 430.0 and 600.1 mm^3. The LinTT1-modified Cyt C& LND lipo exhibited higher tumor inhibition than the Cyt

C&LND group, with tumor size growing from 85.7 to 192.6 mm^3. Blank lipo showed no therapeutic effect since the average tumor size was close to CTRL group. After 14 d treatment, mice were sacrificed, and tumors were extracted. The ex vivo tumor size measured (Figure 5c,d) was consistent with the in vivo data (Figure 5b).

The body weight (Figure 5e) and hepatorenal function parameters (Figure S13, Supporting Information), as well as H&E staining (Figure S14, Supporting Information) of the major organs, were characterized for liposome biosafety analysis. Compared with CTRL and CL lipo group, treatment groups showed body weight decrease during treatment, which may be due to inappetence caused by the treatment. Hematological parameters like aspartate aminotransferase (AST), phenylalanine aminotransferase (ALT), blood urea nitrogen (BUN), and serum creatinine (Cr) were tested (Figure S13, Supporting Information) to evaluate the liver and kidney function. There were no statistically significant changes of Cr between CTRL and lipo groups, but there was a statistically significant increase of ALT, AST, and BUN in LinTT1 lipo group and/or Cyt C&LND lipo group, indicating some interference with kidney and liver function. However, H&E staining of main organs (heart, liver, spleen, lung, kidney) revealed no clear morphological changes or other abnormalities in all groups (Figure S14, Supporting Information). Altogether, these results demonstrated that the Cyt C and/or LND lipo were relatively safe for potential clinical applications.

H&E, TdT-mediated dUTP-biotin nick end labeling (TUNEL) staining, Cyt C, Caspase-7 staining were used to characterize the tumor tissue morphology and apoptosis levels (Figure 5f). For H&E staining, tumors were characterized as dense deep-blue nucleus, and less pink cytoplasm in CTRL and CL lipo group, but tumor cell nucleus shrinked and cytoplasm area increased comparatively in Cyt C lipo and LND lipo group, accompanied by less density of tumor cell, this is the typical features of tumor death. Cyt C and LND combination lipo group exhibited a wider range of tumor ablation than single lipo group. LinTT1 modification aggravated tumor ablation and suppression based on its tumor homing ability.

Apoptosis level was characterized though H&E, Cyt C, and Caspase-7 staining. One of the hallmarks of apoptosis is the generation of free 3′-hydroxyl termini on DNA, the TUNEL assay was able to label the exposed DNA terminals and showed green fluorescence. There were no clear TUNEL marks in CTRL and CL lipo group, while significant TUNEL marks were presented in treatment groups; the Cyt C and LND combination accelerated apoptosis with higher TUNEL level, and apoptosis was further promoted by LinTT1 targeting through higher lipo uptake. The promotion of apoptosis of drug combination may be due to apoptosome assembly as indicated in vitro, instead of elevated Apaf-1 level (Figure S15, Supporting Information). The Cyt C levels within tumor tissues were studied by immunostaining to visualize the Cyt C delivery. Herein, there was a small amount of endogenous Cyt C in tumor tissue in CTRL and CL lipo group, while Cyt C levels increased in Cyt C lipo, Cyt C&LND lipo, as well as LinTT1 lipo group, which correlated with the intracellular Cyt C increase in vitro (Figure 3d), indicating the successful Cyt C delivery both in vitro and in vivo. Caspase-7 was the main effector Caspase during cell apoptosis activated by apoptosome complex. Caspase-7 level showed the similar trend with TUNEL staining, and there was no clear Caspase-7 expression in CTRL and CL lipo group, and Caspase-7 levels elevated from single drug lipo group to drug combination lipo group. Like the TUNEL staining, most tumor cells expressed Caspase-7 in drug combination group and LinTT1 group, indicating the high apoptosis levels of the cells. Balb/c mice were fed under the protocol approved by Animal Experiment Center, Shanghai JiaoTong University (SYXK2022-0009). The animal experiments were in accordance with international ethics guidelines and the National Institutes of Health Guide, concerning the Care and Use of Laboratory Animals.

3. Conclusion

In summary, LinTT1 modified Cyt C and LND co-loaded CL liposomes were prepared as biomimetic nanocarriers for cancer pro-apoptosis therapy. The introduction of CL in the liposomal formulation enhanced Cyt C loading and delivery, while LND reduced the intracellular ATP levels and promoted the cytoplasmic Cyt C binding with Apaf-1, leading to enhanced apoptosome formation and the activation of effector Caspase 3/7 in the downstream of the intrinsic apoptosis pathway. The combination of Cyt C and LND demonstrated significant anti-tumor efficacy both in vitro and in vivo by improving tumor apoptosis levels. Besides, the LinTT1 tumor homing peptide modification further improved the therapeutic effects due to enhanced liposome uptake and accumulation in the tumor site. Overall, the liposomal formulations developed here with a synergistic Cyt C and LND delivery capability provide new insights into cancer therapy targeting apoptosome formation, and thus, making them promising candidates for cancer pro-apoptosis cancer therapy.

4. Experimental Section

The experimental details are reported in the Supporting Information.

Supporting Information

Supporting Information is available from the Wiley Online Library or from the author.

Acknowledgements

H.H. acknowledges financial support from the Chinese Scholarship Council. W.C. acknowledges GuangCi Professorship Program of Ruijin Hospital, Shanghai Jiao Tong University School of Medicine and the National Key Research and Development Program of China (2020YFA0908200). S.W. acknowledges the financial support from the Academy of Finland (Grant No. 331106). H.A.S. acknowledges the Sigrid Jusélius Foundation, the Academy of Finland (Grant No. 331151), and UMCG Research Funds for financial support.

Conflict of Interest

The authors declare no conflict of interest.

Data Availability Statement

The data that support the findings of this study are available from the corresponding author upon reasonable request.

Keywords

apoptosis, apoptosome, cancer therapy, cytochrome c, nanoparticles

Received: May 13, 2023
Revised: June 16, 2023
Published online:

[1] E. Obeng, *Braz. J. Biol.* **2021**, *81*, 1133.
[2] a) C. C. Wu, S. Lee, S. Malladi, M. D. Chen, N. J. Mastrandrea, Z. Zhang, S. B. Bratton, *Nat. Commun.* **2016**, *7*, 13565; b) S. B. Bratton, G. S. Salvesen, *J. Cell Sci.* **2010**, *123*, 3209.
[3] R. Jan, G. E. Chaudhry, *Adv. Pharm. Bull.* **2019**, *9*, 205.
[4] K. M. Hajra, J. R. Liu, *Apoptosis* **2004**, *9*, 691.
[5] a) C. F. A. Warren, M. W. Wong-Brown, N. A. Bowden, *Cell Death Dis.* **2019**, *10*, 177; b) S. D'Aguanno, D. Del Bufalo, *Cells* **2020**, *9*, 1287.
[6] D. Chandra, S. B. Bratton, M. D. Person, Y. Tian, A. G. Martin, M. Ayres, H. O. Fearnhead, V. Gandhi, D. G. Tang, *Cell* **2006**, *125*, 1333.
[7] a) R. Shakeri, A. Kheirollahi, J. Davoodi, *Biochimie* **2017**, *135*, 111; b) H. M. Beere, B. B. Wolf, K. Cain, D. D. Mosser, A. Mahboubi, T. Kuwana, P. Tailor, R. I. Morimoto, G. M. Cohen, D. R. Green, *Nat. Cell Biol.* **2000**, *2*, 469; c) P. Pandey, A. Saleh, A. Nakazawa, S. Kumar, S. M. Srinivasula, V. Kumar, S. Kharbanda, *EMBO J.* **2000**, *19*, 4310; d) C. Garrido, E. Solary, *Cell Death Differ.* **2003**, *10*, 619.
[8] a) I. M. Melzer, S. B. Fernandez, S. Bosser, K. Lohrig, U. Lewandrowski, D. Wolters, S. Kehrloesser, M. L. Brezniceanu, A. C. Theos, P. M. Irusta, F. Impens, K. Gevaert, M. Zornig, *Cell Death Differ.* **2012**, *19*, 1435; b) X. Qi, L. Wang, F. Du, *Biochemistry* **2010**, *49*, 1923; c) M. Eissmann, I. M. Melzer, S. B. Fernandez, G. Michel, M. Hrabe de Angelis, G. Hoefler, P. Finkenwirth, A. Jauch, B. Schoell, M. Grez, M. Schmidt, C. C. Bartholomae, S. Newrzela, N. Haetscher, M. A. Rieger, C. Zachskorn, M. Mittelbronn, M. Zornig, *Oncogene* **2013**, *32*, 2586.
[9] R. Kumar, T. A. Bhat, E. M. Walsh, A. K. Chaudhary, J. O'Malley, J. S. Rhim, J. Wang, C. D. Morrison, K. Attwood, W. Bshara, J. L. Mohler, N. Yadav, D. Chandra, *Cancer Res.* **2019**, *79*, 1353.
[10] Q. Wang, C. Chen, X. Xu, C. Shu, C. Cao, Z. Wang, Y. Fu, L. Xu, K. Xu, J. Xu, A. Xia, B. Wang, G. Xu, X. Zou, R. Su, W. Kang, Y. Xue, R. Mo, B. Sun, S. Wang, *Adv. Sci.* **2022**, *9*, 2201889.
[11] a) S. K. Kim, M. B. Foote, L. Huang, *Biomaterials* **2012**, *33*, 3959; b) S. Li, J. Zhang, C. Deng, F. Meng, L. Yu, Z. Zhong, *ACS Appl. Mater. Interfaces* **2016**, *8*, 21155; c) X. S. Sun, M. S. Jang, Y. Fu, J. H. Lee, D. S. Lee, Y. Li, H. Y. Yang, *Mater. Sci. Eng., C* **2020**, *114*, 111069; e) J. Mendez, M. Morales Cruz, Y. Delgado, C. M. Figueroa, E. A. Orellano, M. Morales, A. Monteagudo, K. Griebenow, *Mol. Pharm.* **2014**, *11*, 102; f) E. Choi, D. K. Lim, S. Kim, *J. Colloid Interface Sci.* **2020**, *560*, 416; g) V. Barcelo-Bovea, I. Dominguez-Martinez, F. Joaquin-Ovalle, L. A. Amador, E. Castro-Rivera, K. Medina-Alvarez, A. McGoron, K. Griebenow, Y. Ferrer-Acosta, *Cancers* **2020**, 12; h) H. Y. Yang, J. Meng Du, M. S. Jang, X. W. Mo, X. S. Sun, D. S. Lee, J. H. Lee, Y. Fu, *Biomacromolecules* **2021**, *22*, 3590; i) L. Ding, Y. Jiang, J. Zhang, H. A. Klok, Z. Zhong, *Biomacromolecules* **2018**, *19*, 555.
[12] a) M. Akram, *J. Cancer Educ.* **2013**, *28*, 454; b) D. Cervantes-Madrid, A. Duenas-Gonzalez, *Oncol. Rep.* **2015**, *34*, 1533.
[13] V. Andra, S. V. N. Pammi, L. Bhatraju, L. K. Ruddaraju, *J. Bionanosci.* **2022**, *12*, 274.
[14] P. P. M. Pizzuto, *Trends Cell Biol.* **2020**, *30*, 892.
[15] M. Rytömaa, P. K. Kinnunen, *J. Biol. Chem.* **1994**, *269*, 1770.
[16] S. L. Iverson, S. Orrenius, *Arch. Biochem. Biophys.* **2004**, *423*, 37.
[17] a) V. Fogal, L. Zhang, S. Krajewski, E. Ruoslahti, *Cancer Res.* **2008**, *68*, 7210; b) H. Hunt, L. Simon-Gracia, A. Tobi, V. R. Kotamraju, S. Sharma, M. Nigul, K. N. Sugahara, E. Ruoslahti, T. Teesalu, *J. Control Release* **2017**, *260*, 142; c) G. Torrieri, F. Fontana, P. Figueiredo, Z. Liu, M. P. A. Ferreira, V. Talman, J. P. Martins, M. Fusciello, K. Moslova, T. Teesalu, V. Cerullo, J. Hirvonen, H. Ruskoaho, V. Balasubramanian, H. A. Santos, *Nanoscale* **2020**, *12*, 2350.
[18] R. Cheng, F. Fontana, J. Xiao, Z. Liu, P. Figueiredo, M. A. Shahbazi, S. Wang, J. Jin, G. Torrieri, J. T. Hirvonen, H. Zhang, T. Chen, W. Cui, Y. Lu, H. A. Santos, *ACS Appl. Mater. Interfaces* **2020**, *12*, 44554.
[19] V. E. Kagan, H. A. Bayır, N. A. Belikova, O. Kapralov, Y. Y. Tyurina, V. A. Tyurin, J. Jiang, *Free Radical Biol. Med.* **2009**, *46*, 1439.
[20] P. Nakhaei, R. Margiana, D. O. Bokov, W. K. Abdelbasset, M. A. Jadidi Kouhbanani, R. S. Varma, F. Marofi, M. Jarahian, N. Beheshtkhoo, *Front. Bioeng. Biotechnol.* **2021**, *9*, 705886.
[21] a) Z. Zhao, A. Ukidve, V. Krishnan, Mitragotri, *Adv. Drug Delivery Rev.* **2019**, *143*, 3; b) Y. Wang, X. Ma, W. Zhou, C. Liu, H. Zhang, *Smart Med.* **2022**, *1*, 1; c) W. Zhou, X. Ma, J. Wang, X. Xu, O. Koivisto, J. Feng, T. Viitala, H. Zhang, *Smart Med.* **2022**, *1*, e20220036; d) Y. Ding, C. Liu, Y. Wu, F. Fu, *Biomed. Technol.* **2023**, *4*, 41; e) Q. Zhang, G. Kuang, L. Zhang, Y. Zhu, *Biomed. Technol.* **2023**, *2*, 77; f) H. Han, J. Li, H. A. Santos, *Biomed. Technol.* **2023**, *3*, 40; g) R. Cheng, S. Wang, H. A. Santos, *Biomed. Technol.* **2023**, *3*, 52.
[22] C. Corbo, R. Molinaro, F. Taraballi, N. E. Toledano Furman, M. B. Sherman, A. Parodi, F. Salvatore, E. Tasciotti, *Int. J. Nanomed.* **2016**, *11*, 3049.
[23] D. Pozzi, G. Caracciolo, L. Digiacomo, V. Colapicchioni, S. Palchetti, A. L. Capriotti, C. Cavaliere, R. Zenezini Chiozzi, A. Puglisi, A. Laganà, *Nanoscale* **2015**, *7*, 13958.
[24] P. Bharmoria, T. J. Trivedi, A. Pabbathi, A. Samanta, A. Kumar, *Phys. Chem. Chem. Phys.* **2015**, *17*, 10189.
[25] a) J. Hanske, J. R. Toffey, A. M. Morenz, A. J. Bonilla, K. H. Schiavoni, E. V. Pletneva, *Proc. Natl. Acad. Sci. USA* **2012**, *109*, 125; b) M. M. Elmer-Dixon, Z. Xie, J. B. Alverson, N. D. Priestley, B. E. Bowler, *J. Am. Chem. Soc.* **2020**, *142*, 19532.
[26] N. d'Avanzo, G. Torrieri, P. Figueiredo, C. Celia, D. Paolino, A. Correia, K. Moslova, T. Teesalu, M. Fresta, H. A. Santos, *Int. J. Pharm.* **2021**, *597*, 120346.
[27] C. Langlais, M. A. Hughes, K. Cain, M. MacFarlane, *Cold Spring Harb Protoc.* **2015**, *2015*, 1069.
[28] L. Ravagnan, I. Marzo, P. Costantini, S. A. Susin, N. Zamzami, P. X. Petit, F. Hirsch, M. Goulbern, M.-F. Poupon, L. Miccoli, Z. Xie, J. C. Reed, G. Kroemer, *Oncogene* **1999**, *18*, 2537.
[29] K. Nath, L. Guo, B. Nancolas, D. S. Nelson, A. A. Shestov, S. C. Lee, J. Roman, R. Zhou, D. B. Leeper, A. P. Halestrap, I. A. Blair, J. D. Glickson, *Biochim. Biophys. Acta* **2016**, *1866*, 151.
[30] S. Sharma, V. R. Kotamraju, T. Molder, A. Tobi, T. Teesalu, E. Ruoslahti, *Nano Lett.* **2017**, *17*, 1356.